Self-avoiding walks in four dimensions: logarithmic corrections

1994 J. Phys. A: Math. Gen. 27 7265

(http://iopscience.iop.org/0305-4470/27/22/006)

J. Phys. A: Math. Gen. 27 (1994) 7265–7282. Printed in the UK

Self-avoiding walks in four dimensions: logarithmic corrections

Peter Grassberger†, Rainer Hegger† and Lothar Schäfer‡

† Physics Department, University of Wuppertal, D-42 097 Wuppertal, Germany
‡ Physics Department, University of Essen, D-45 117 Essen, Germany

Received 15 July 1994, in final form 16 September 1994

Abstract. We present simulation results for long ($N \leqslant 4000$) self-avoiding walks in four dimensions. We find definite indications of logarithmic corrections, but the data are poorly described by the asymptotically leading terms. Detailed comparisons are presented with renormalization-group flow equations derived by direct renormalization and with the results of a field-theoretic calculation.

1. Introduction

Self-avoiding walks (SAWs) are of practical importance since they form a model for randomly coiled linear polymers, but even more important for theoretical physics is that they represent, in some sense, the simplest critical phenomenon. More precisely, they are formally described by the $m \to 0$ limit of the O(m) Landau–Ginzburg field theory [1]. Other members of this family are the Ising ($m = 1$) and the Heisenberg ($m = 3$) models.

The most profound theoretical understanding of these critical phenomena is obtained by the field-theoretic renormalization group evaluated near four dimensions. Above $d = 4$, all O(m) models show mean-field behaviour. Below $d = 4$, the deviations of the critical exponents from their mean-field values are of order $\epsilon = 4 - d$. This follows from the fact that the renormalized coupling constant is of order ϵ in the infra-red limit. The most extensively studied method for estimating critical exponents (the 'ϵ-expansion') involves resumming perturbation expansions in ϵ. Precisely at $d = 4$, the deviation from mean-field behaviour is given by logarithmic corrections which can be predicted unambiguously by renormalization theory. Specifically, the leading behaviour in the limit of long chains is [1]

$$R_N^2 \sim N\,[\log N]^{\alpha} \qquad \alpha = \tfrac{1}{4} \tag{1}$$

for the average squared end-to-end distance, and

$$C_N \sim \mu^N [\log N]^{\beta} \qquad \beta = \tfrac{1}{4} \tag{2}$$

for the number of distinct walks. These predictions are basic results. In particular, they do not suffer from any ambiguities inherent in a resummation of the ϵ-expansion. Thus it would be extremely useful if one could verify them by independent means. The most obvious candidates for alternative calculations are exact enumerations of short walks and Monte Carlo simulations. Both methods have been applied previously.

Enumerations of chains with lengths of up to $N = 18$ have been used in [2–4] to verify (2) (R_N was not computed in these papers), and recently chains were enumerated with N

0305-4470/94/227265+18$19.50

up to $N = 21$ [5]. From this the authors claim excellent agreement with (2): the power of the logarithm in the best fit is $\beta = 0.250 \pm 0.005$.

Monte Carlo simulations, on the other hand, have been used previously for estimating α in [6, 9]. In addition, different exponents related to α and β were measured in [7, 8]. While [6–8] claim good agreement with (1) (with, for example, $\alpha = 0.25 \pm 0.02$ in [6]) and with (2), serious disagreement was found in [9], where the best fit was obtained with $\alpha = 0.31$. Although no error bars were given in [9], the author obviously considered the value $\alpha = \frac{1}{4}$ to be ruled out. This seems a serious problem since the simulations of [9] are more significant statistically by far than those of [6–8], both concerning the chain lengths (N up to 2400) and the sample size. Also, the method of analysis used in [6] was justly criticized in [9] since it introduced an uncontrolled bias and did not use the data optimally.

The methods used in [7, 8] (in both papers, identical methods were used) are not easily compared to the present one. In different runs, these authors measured the average length $\langle N_R \rangle_p$ of chains with fixed end-to-end distance R in grand canonical ensembles at $p < p_c$ (p is the fugacity), and the probability $Q(p)$ that two chains starting at neighbouring sites never cross each other. We have not measured $Q(p)$ ourselves (such measurements will be presented in [10]), but we have measured $\langle N_R \rangle_p$. From this we shall argue in section 5 that the analyses of [7, 8] have large systematic errors, and, indeed, that deviations from mean-field behaviour are much larger than claimed there.

In view of this situation (and since simulations of theta polymers in three dimensions [11] also gave discrepancies with the logarithmic corrections expected [1]) we decided to perform simulations with much higher accuracy than those done previously.

We find that the numerical results of [9] are correct (though we do not agree with the conclusions drawn from them). In contrast, it seems that the findings of [6–8] were not completely uneffected by wishful thinking. This means that the leading logarithmic terms of (1) and (2) are not sufficient to describe the behaviour at any chain lengths which can be simulated in the foreseeable future (unless we assume, as was done in [9], that the leading terms show a different power of $\log N$).

The first corrections to the asymptotic laws (equations (1) and (2)) have been calculated by Duplantier [12], but it turns out that even the corrected expressions are not fully consistent with the numerical data. These expressions involve a non-universal parameter (an integration constant from integrating the renormalization-group flow) which should be the same for R_N^2 and C_N. But for a good fit two different values have to be chosen for R_N^2 and C_N, which is an internally inconsistent procedure. However, from our data we can extract logarithmic derivatives $\partial \ln R_N^2 / \partial \ln N$ and $\partial \ln C_N / \partial \ln N$, which may be compared directly to renormalization-group flow equations of an appropriate direct renormalization scheme. Such a comparison does not involve unknown fit parameters. It is thus very pleasing that the flow equations can consistently be put into a form which compares very well with our Monte Carlo data.

Stimulated by that success we use the original data to test another theoretical approach. As has been stressed previously [13, 14], the renormalization approach can be viewed as proceeding in two essentially independent steps. We first determine a mapping from the physical model to its renormalized counterpart, and in a second step we use renormalized perturbation theory to determine the observables, working completely within the renormalized model. It has been suggested that the mapping must be determined most precisely, but in the second step we may be content with low-order perturbation theory. We find that this method allows for a consistent determination of the non-universal parameters and yields a good quantitative fit to our data.

The paper is organized as follows: in the next section we present our Monte Carlo

algorithm and the resulting data. Comparison with renormalization-group flow equations derived in the spirit of direct renormalization is given in section 3, while comparison with field-theoretic renormalization is presented in section 4. We conclude with a discussion of our results in section 5.

2. Simulations

Aiming at estimates for both R_N^2 and C_N, we decided not to use the pivot algorithm [16], though it should be the most efficient algorithm for estimating R_N in the limit $N \to \infty$. Instead, we used a recursive and randomized implementation of the old enrichment method [17]. This method is an improvement over the incomplete enumeration or 'recursive sampling' method used in [18, 19], and was applied successfully in [11, 20] to polymer adsorption on surfaces, to theta polymers and to off-lattice polymers interacting via Lennard-Jones potentials.

The basic structural element of incomplete enumeration is a subroutine STEP(x) which marks the site x as occupied and calls itself at all neighbouring sites $x \pm e_i$, provided these sites are still free and provided $N < N_{\max}$. Before leaving the subroutine, the site x is marked as free again. If each free neighbouring site were visited with probability 1, this would give exact enumeration. In order to obtain a grand canonical distribution of walks where

$$n_N = \text{constant} \times C_N p^N \tag{3}$$

is the average number of N-step walks, one has to use a random number generator so that only a fraction p of all free neighbours are visited.

The basis of the present improvement is the observation that it is sufficient to visit only one of the neighbours (provided it is free; otherwise the subroutine is left immediately), but on average $(\mathcal{N}-1)p$ times. Here $\mathcal{N}$ is the coordination number of the lattice, and we have assumed that we do not attempt any back steps as the corresponding site would not be free anyway. The average chain length diverges when $p \to p_c = 1/\mu$. Since $(\mathcal{N}-1)p_c > 1$ for all lattices, this means that we make > 1 attempts to continue each successful path if $p \approx p_c$. Thus we choose a random neighbour (different from that we had come from), call STEP at this neighbour, and after having returned we call STEP again at the same neighbour with probability $(\mathcal{N}-1)p_c - 1$. The main difference to the algorithm of [21], for example, is that we always try at least once to continue the walk.

Like the incomplete enumeration method of [18, 19] and like the method of [21], the present method corresponds essentially to a random walk in the chain length with reflecting boundary conditions at $N = 0$ and $N = N_{\max}$. At p_c, it takes thus roughly N^2/D steps to obtain one statistically independent SAW of length N. Here D is a diffusion constant which is of order unity in the algorithms of [18, 21, 19]. The main advantage of the present algorithm (apart from slightly shorter programs) is that here

$$D \sim 1/\delta \qquad \delta = ((\mathcal{N}-1)p_c - 1)\,. \tag{4}$$

Since $\delta \approx 0.033$ for the simple hypercubic lattice in $d = 4$, this gives a very large diffusion coefficient, and the method is more than one order of magnitude faster than those of [18, 21, 19]. Equation (4) can be understood as follows: in the present algorithm, a step back in N is only needed when the walker hits an occupied site. The chance for this is $\approx \delta$. In simulations near p_c, this means that on average $1/\delta$ forward steps are made until one

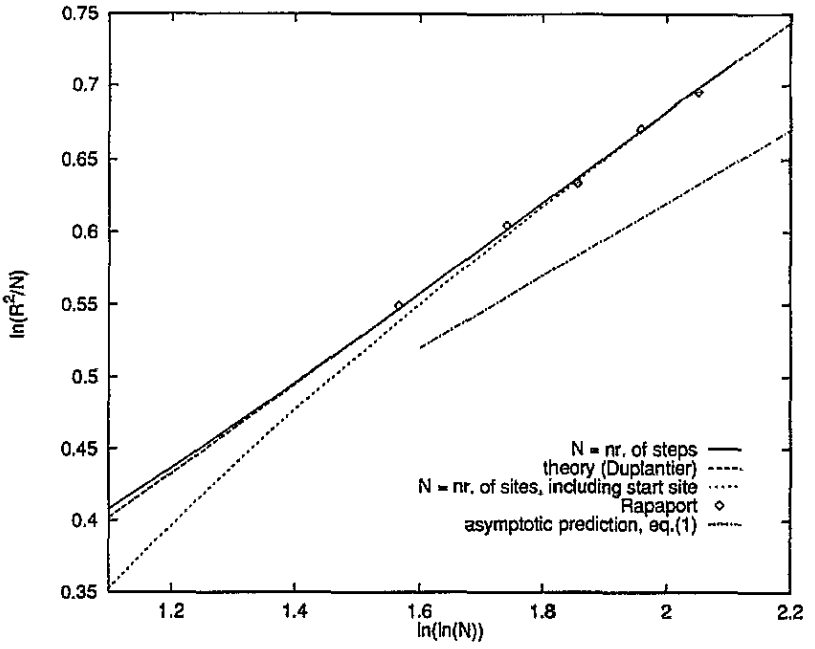

Figure 1. Plot of the logarithm of the swelling ratio, $\ln(R_N^2/N)$, against $\ln(\ln N)$. The full curve shows our data with N taken as the number of bonds; the dotted curve represents these data with N as the number of sites. The diamonds are the data from [9], and the dashed curve is the fit with (5). The chain curve indicates the slope predicted by the leading term given in (1). The statistical errors of our data are roughly $\propto \sqrt{N}$. They are thus largest for $N = 4000$, where $\Delta \ln R_N^2 = 0.0005$.

back jump reduces N by $1/\delta$. In each of [18, 21, 19], in contrast, the probability to make a back step is of order 1 (it is $(1-p)^\mu$ for [18, 19], and $1/(1+p\mathcal{N})$ for [21]).

We have simulated SAWs of length up to $N_{\max} = 4000$. Since it is not possible to store the sites occupied by such long walks in a simple bit map, we used a hashing procedure similar to (but somewhat simpler than) that used in [16]. We made only simulations very close to p_c, where n_N is roughly independent of N. As explained in [17, 19], this should be most efficient. Our total sample corresponded to $n_N \approx 10^8$. This is also roughly the number of SAWs of maximal length $N_{\max}$, but all these walks are, of course, not independent. Often it is stated that this correlation between the walks is the main drawback of the enrichment method. In our version, it is not a big problem because of the ease with which walks are generated. The number of independent walks is given by the number of instances where the algorithm has reached $N = N_{\max}$ between two returns to the main routine (corresponding to $N = 0$). Our sample contained $\approx 1.2 \times 10^6$ such independent walks. The total CPU time was ~800 h on a cluster of DEC ALPHA workstations.

Our results for R_N^2/N are shown in figure 1. In order to compare with (1), we plotted its logarithm against $\ln(\ln N)$. To demonstrate the importance of non-leading terms in logarithmic expressions, we show two slightly different quantities. For the full curve, N is defined as the number of *bonds*, while N is the number of *sites* for the dotted curve. These two definitions differ by one unit and are clearly equivalent for $N \to \infty$. Nevertheless, we see that the difference is still important for $N = 300$! We

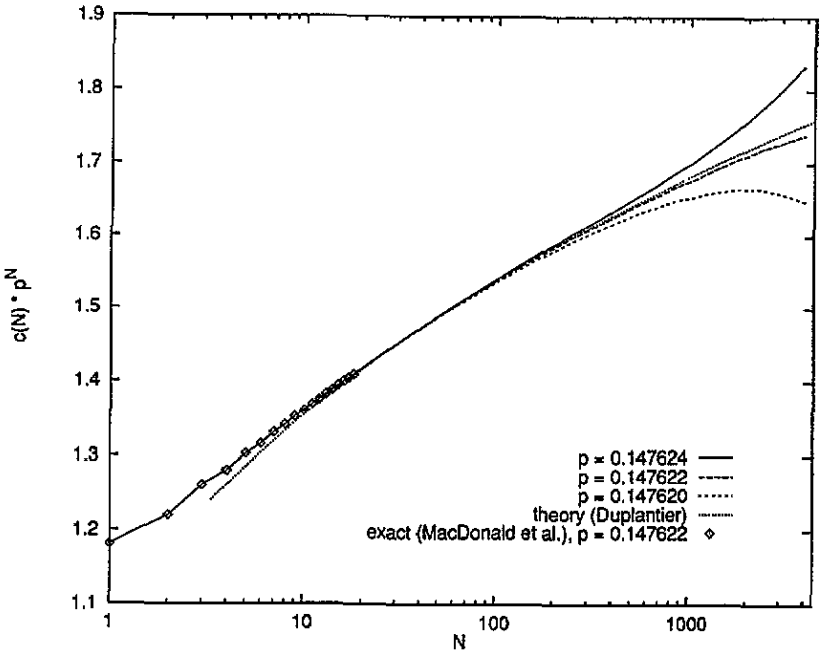

Figure 2. Semi-logarithmic plot of $C_N p^N$ against $\ln N$. The plot shows our MC data for three different values of p very near p_c, the fit with (6), and the exact enumeration data from [4]. The statistical error of our data for $N = 4000$ is $\Delta C_N / C_N = 0.0013$.

also show the results of [9] which have larger error bars but are otherwise in perfect agreement. From (1) we expect our data to fall onto a straight line with slope $\frac{1}{4}$. This is definitely not seen. Instead, the best straight line to the data (where N is interpreted as the number of bonds) has slope 0.311 ± 0.003. It would indeed give a perfectly acceptable fit.

Our data for C_N are shown in figure 2. More precisely, there we plotted $C_N p^N$ against $\ln N$ for three different values of p. We also show the exact enumeration data of [4] with which we are in perfect agreement. But again we see hardly any sign of the predicted asymptotic behaviour. We do not want to discuss in detail why several authors [2–4] were able to extract the correct asymptotic behaviour from enumeration data (for noiseless data there exist very sophisticated methods to extract singularities), but obviously non-leading contributions are very large.

3. Higher-order terms and renormalization-group flow

Fortunately, the leading corrections to (1) and (2) have been calculated in [12]

$$\alpha_N \equiv R_N^2/N = r[\ln(N/a)]^{1/4}\left[1 - \frac{17\ln(4\ln(N/a)) + 31}{64\ln(N/a)} + \ldots\right] \tag{5}$$

$$C_N/\mu^N = c[\ln(N/a)]^{1/4}\left[1 - \frac{17\ln(4\ln(N/a)) - 3}{64\ln(N/a)} + \ldots\right]. \tag{6}$$

Here the constant a has to be treated as a free parameter. We thus have two parameters (r, a) to fit R_N^2/N, and two more (μ, c) if we also want to fit C_N.

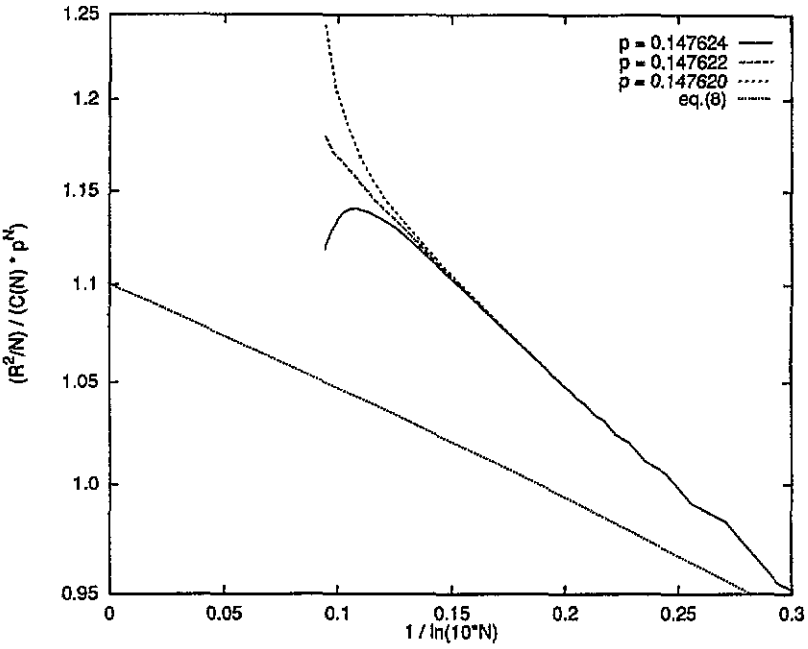

Figure 3. Plot of $(R_N^2/N)/(C_N p^N)$ against $1/\ln(10N)$. According to (7) a straight line with negative slope is expected for $p = p_c$, with a slope as indicated by the dotted line.

The best fit to (5) is obtained with $r = 1.331, a = 0.1237$. It is included in figure 1 (broken curve). Over the range of interest it practically is undistinguishable from a straight line with slope 0.311.

For C_N it is even more obvious that the leading term $[\ln(N/a)]^{1/4}$ would give a very poor fit. A fit with (6), again using a as a free parameter, gives $c = 1.05$ and $a = 0.055$. This fit is shown as a dotted line in figure 2. Notice that the values of a extracted from α_N and from C_N differ considerably. No acceptable fit is found with a common value of a.

Neglecting this problem for the moment, our data suggest that the critical value of p is $p_c = 0.147\,622 \pm 0.000\,001$. This is to be compared to $p_c = 0.147\,625 \pm 0.000\,002$ as obtained in [5]. The values accepted in [7, 8] were substantially larger, 0.1490 ± 0.0003 and 0.1493 ± 0.0007, which partly explains why smaller logarithmic corrections were found in these papers (see section 5).

We have thus been able to produce individual good fits to R_N^2/N and to $C_N p^N$, but the non-leading corrections are very important (in the latter case masking completely the leading behaviour), and the fit parameters are not mutually consistent. This can also be seen by plotting the ratio $(R_N^2/N)/(C_N p^N)$. Here the dominant terms cancel, and we obtain

$$\frac{\alpha_N}{C_N p_c^N} = \text{constant} \times \left[1 - \frac{17}{32\ln(N/a)} + \ldots\right]. \tag{7}$$

From figure 3 we see that this ratio is indeed a roughly linear function of $1/\ln(N/a)$, provided we take $a \approx 0.1$. The slope of this function has the right sign but is roughly twice as large as the value predicted by (7). To summarize, even including the leading correction terms we do not find a fully satisfactory explanation of the data.

To proceed we note that (5) and (6) are derived by integrating the renormalization-group flow equations, keeping only terms up to one loop order. It therefore is of interest to take a step back and compare the data against the more basic flow equations. We first reconstruct the flow equations from results given in the literature.

Following [15], we start from dimensionally regularized perturbation theory in $d = 4-\epsilon$ dimensions. Denoting by b the bare coupling constant and by

$$z = \frac{bN^{\epsilon/2}}{(2\pi)^{d/2}} \tag{8}$$

a dimensionless coupling strength, we have up to second order in z [15]

$$\alpha_N = 1 + z\left(\frac{2}{\epsilon} - 1\right) + z^2\left(-\frac{6}{\epsilon^2} + \frac{11}{2\epsilon}\right) + \mathcal{O}(z^3) \tag{9}$$

$$C_N/\mu^N = 1 + z\left(\frac{1}{\epsilon} + \frac{1}{2}\right) - z^2\left(\frac{7}{2\epsilon^2} + \frac{4}{\epsilon}\right) + \mathcal{O}(z^3)\,. \tag{10}$$

Obviously these expansions are singular at $d \to 4$. We thus introduce a renormalized coupling constant, which in the minimal subtraction scheme of [22] reads

$$z_R = z - \frac{8}{\epsilon}z^2 + \left(\frac{64}{\epsilon^2} + \frac{17}{\epsilon}\right)z^3 + \mathcal{O}(z^4)\,. \tag{11}$$

From this we get the Wilson function [12]

$$W[z_R, \epsilon] = N\frac{\partial}{\partial N} z_R|_{b,\epsilon} = \tfrac{1}{2}\epsilon z_R - 4z_R^2 + 17z_R^3 + \cdots \tag{12}$$

in which we can take the limit $\epsilon \to 0$ without encountering any problems:

$$W[z_R] = -4z_R^2 + 17z_R^3 + \mathcal{O}(z_R^4)\,. \tag{13}$$

While α_N or C_N/μ^N expressed in terms of z_R still are singular, their derivatives with respect to $\ln N$ are known to be finite. Indeed these derivatives yield flow equations governing the renormalization of the chain length and of the partition function. Defining

$$\sigma_0[z_R, \epsilon] = N\frac{\partial \ln \alpha_N}{\partial \ln N}\Big|_{b,\epsilon} \tag{14}$$

and

$$\sigma_1[z_R, \epsilon] = N\frac{\partial \ln C_N}{\partial \ln N}\Big|_{b,\epsilon} \tag{15}$$

we have [12]

$$\sigma_0[z_R] = \lim_{\epsilon\to 0}\sigma_0[z_R, \epsilon] = z_R + \tfrac{7}{2}z_R^2 + \cdots \tag{16}$$

$$\sigma_1[z_R] = \lim_{\epsilon\to 0}\sigma_1[z_R, \epsilon] = z_R - 5z_R^2 + \cdots\,. \tag{17}$$

Equations (5) and (6) were obtained by first integrating (12) at $\epsilon = 0$, yielding z_R as a function of N. This was inserted into (16) (respectively (17)), and (14) (respectively (15)) were integrated again. During these manipulations, only the leading terms were kept, since higher-order terms are not completely known.

Avoiding these integrations we now directly compare our data to (12)–(17). We first calculate the derivatives (14) and (15) as functions of N. Of course, we have to replace derivatives with respect to N by finite differences (we use $\Delta \ln N = \ln 2$ for first derivatives, and $\ln 4$ for second), but this should not present many problems in view of the slow variations of all functions involved.

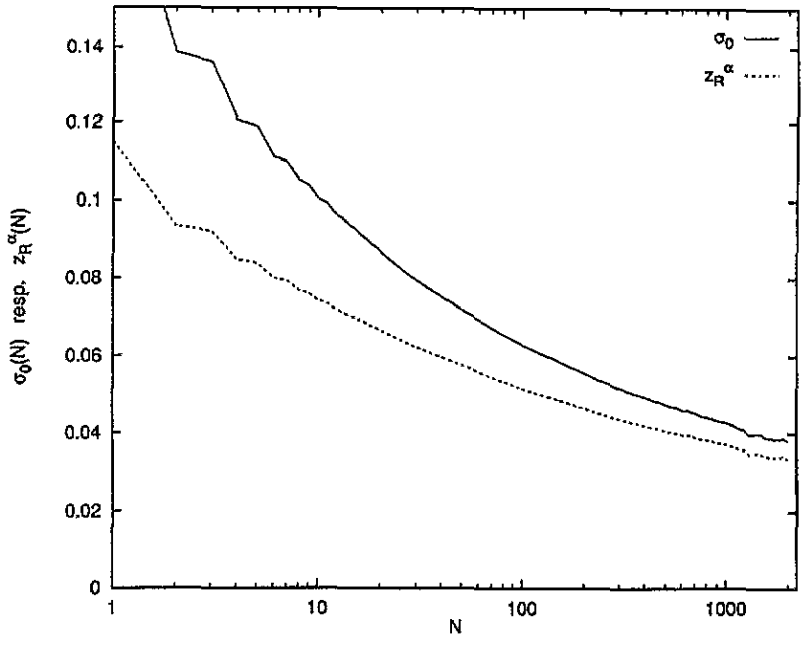

Figure 4. Function $\sigma_0(N)$ against N (full curve). Also shown is $z_R^{(\alpha)}(N)$ as obtained by the Padé approximant (22) (broken curve).

Thus we show in figure 4

$$\sigma_0(N) \equiv \frac{1}{\ln 2} \ln \frac{R_{2N}^2}{2R_N^2} \tag{18}$$

while

$$\sigma_1(N, p) \equiv \frac{1}{\ln 2} \ln \frac{p^N C_{2N}}{C_N} \tag{19}$$

is plotted in figure 5 for the same three values of p as before. From these plots, we should be able to obtain the same function $z_R(N)$ by inverting (16) and (17). A quick test shows that this is not so easy. The problem is that $z_R(N)$ turns out to be not very small (even for the largest values of N), and the Taylor expansions (16) and (17) obviously are poorly convergent. This is particularly true for σ_1, for which truncation in (17) after the quadratic term yields $\sigma_1 \leqslant 0.05$, in contradiction to the data for $N < 30$.

A trick which helps—though its justification is far from obvious—is to change the expansions in (14) and (17) into Padé approximants,

$$\sigma_0[z_R] = \frac{z_R}{1 - \frac{7}{2} z_R} \qquad \sigma_1[z_R] = \frac{z_R}{1 + 5 z_R}. \tag{20}$$

These can be inverted to give

$$z_R = z_R^{(\alpha)} = z_R^{(C)} \tag{21}$$

with

$$z_R^{(\alpha)} = \frac{\sigma_0}{1 + \frac{7}{2}\sigma_0} \qquad z_R^{(C)} = \frac{\sigma_1}{1 - 5\sigma_1}. \tag{22}$$

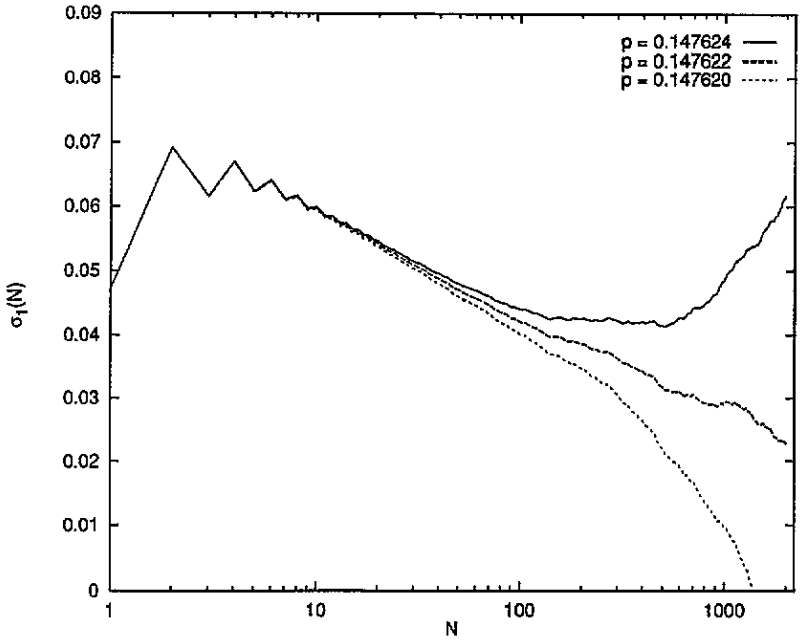

Figure 5. Function $\sigma_1(N)$ against N, for the same three values of p as in figure 2.

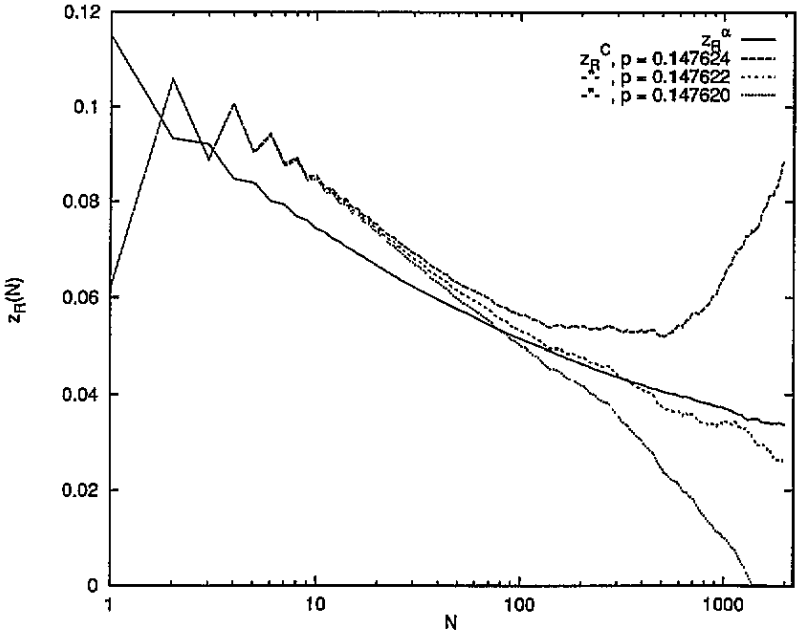

Figure 6. Functions $z_R^{(\alpha)}(N)$ (full curve) and $z_R^{(C)}$ (broken curve). The latter is again shown for the same three values of p.

In figure 6 we have plotted $z_R^{(\alpha)}$ and $z_R^{(C)}$ as obtained from the finite-difference approximations. We still see some disagreement for small N which may be due to higher-

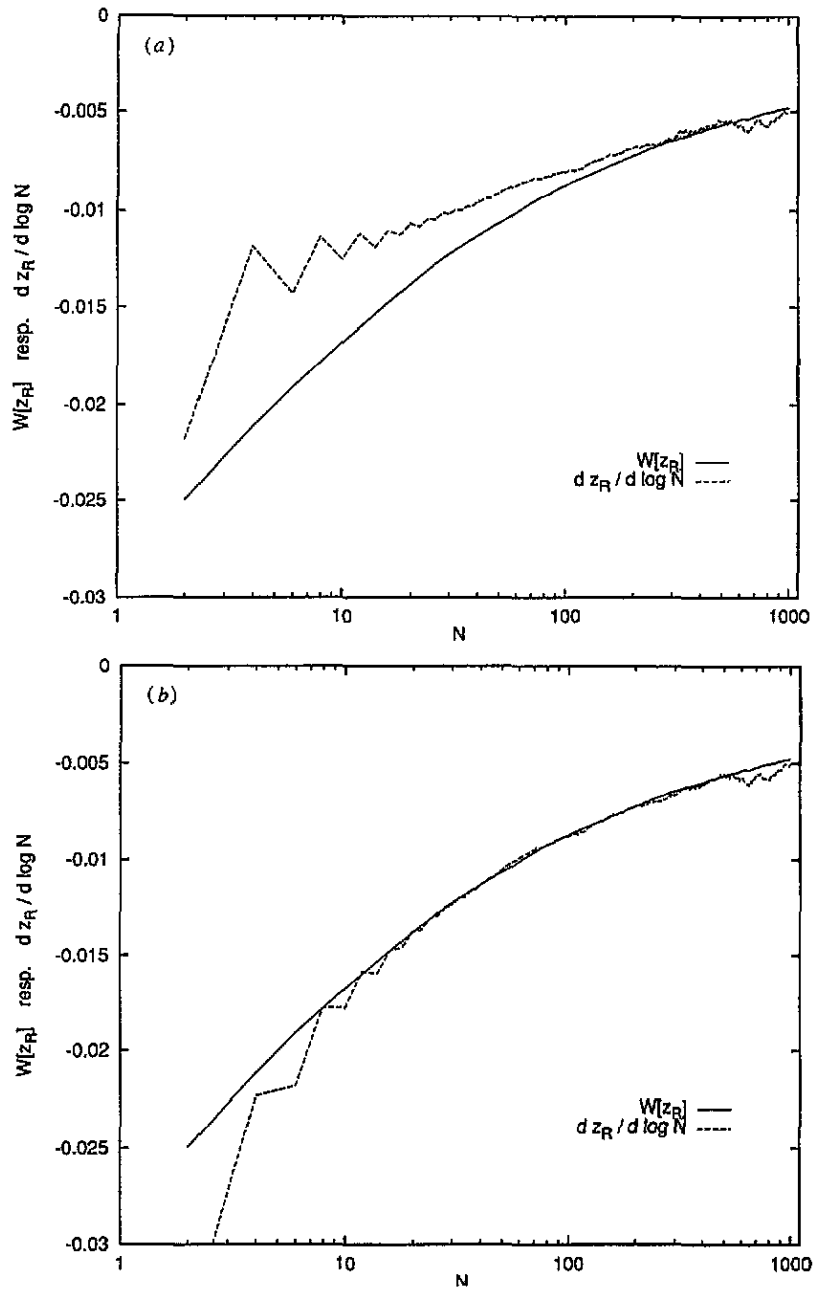

Figure 7. (*a*) Function $W[z_R^{\alpha}]$ (full curve) and the 'derivative' of z_R^{α} with respect to $\ln N$ (broken curve). Both curves should agree up to higher orders in z_R. (*b*) Shows the same data, but in the definition of α_N we have replaced N by $N + 0.17$.

order terms in $\sigma_0[z_R], \sigma_1[z_R]$ and/or to $1/N$ corrections. But for large N we find very acceptable agreement, provided we take $p = 1/\mu = 1.476\,223$.

The final test of the theory consists in checking whether these estimates of z_R satisfy the differential equation $N\,dz_R/dN = W[z_R]$ or, rather, its finite-difference approximation.

Again we find problems due to the slow convergence of the Taylor expansion for $W[z_R]$, and again we take recourse to a Padé approximant

$$W[z_R] = -\frac{4z_R^2}{1+\frac{17}{4}z_R}. \tag{23}$$

In figure 7(*a*) we have plotted this form of W with argument $z_R^{(\alpha)}$ against N, together with

$$\frac{\Delta z_R^{(\alpha)}(N)}{\Delta \ln N} = \frac{z_R^{(\alpha)}(2N) - z_R^{(\alpha)}(N/2)}{\ln 4}. \tag{24}$$

We see very good agreement, in particular, for large values N where it is most significant. For small N agreement could indeed be improved by adding a constant of $\mathcal{O}(1)$ to N so that α_N is replaced by $R_N^2/(N+0.16)$, see figure 7(*b*). Such a $1/N$ correction would also improve the agreement in figure 6 at intermediate values of N.

We thus conclude that our data are fully consistent with the renormalization-group flow predicted theoretically, though there is some ambiguity related to the use of Padé approximants and—to a much lesser degree—to the treatment of $1/N$ corrections. We want to stress that this analysis is particularly interesting since, except for the size of the non-universal $1/N$ corrections, it does involve no fit parameter! Note further, that this analysis uses only the information underlying also (5) or (6). This suggests that solving the renormalization-group equations to one-loop order and substituting the result into expressions for higher-order corrections we lose meaningful information which still can be identified on the level of the flow equations.

4. Field-theoretic renormalization

As mentioned in the introduction, the renormalization program may be separated into two steps: we first map the physical 'bare' model on a renormalized model which exhibits the scale invariance of long chains. We then calculate R_N^2, C_N perturbatively within the renormalized model.

The bare model depends on the coupling constant b, the chain length N, and a microscopic length scale l which is of the order of the lattice spacing in the computer experiments. In the renormalized theory these parameters are replaced by the renormalized coupling u, the renormalized chain length N_R, and a renormalized length scale l_R. The mapping takes the general form

$$b = \text{constant} \times \left(\frac{l}{l_R}\right)^{\epsilon} Z_u(u, l/l_R)u \tag{25}$$

$$N = \left(\frac{l_R}{l}\right)^2 Z_n(u, l/l_R)N_R \tag{26}$$

where the renormalization factors are normalized according to

$$Z_u(0,1) = Z_n(0,1) = 1. \tag{27}$$

The observables of interest here can be expressed as

$$R_N^2 = 2dl_R^2 N_R A_R(u, N_R) \tag{28}$$

$$\frac{C_N}{\mu^N} = \text{constant} \times \frac{Z(u, l/l_R)}{Z_n(u, l/l_R)} A_C(u, N_R) \tag{29}$$

where $Z(\cdots)$ denotes another renormalization factor and the amplitudes A_R, A_C are to be calculated by renormalized perturbation theory. In general, the renormalization factors have to be chosen to absorb the leading dependence on the microscopic scale l: for fixed l_R, all observables have to become independent of l up to corrections of order $l^2/l_R^2 N_R \sim 1/N$. Using the scheme of dimensional regularization, defined by taking the limit $l \to 0$ for $d < 4$, factors such as to make the renormalized theory finite in four dimensions.

The length scale l_R is a free parameter of the renormalized theory. Under a change of l_R the other parameters change according to the flow equations

$$\frac{\partial u}{\partial \ln l_R} = \epsilon u - \tilde{\beta}(u) \tag{30}$$

$$\frac{\partial \ln Z_n}{\partial \ln l_R} = \zeta_n(u) \tag{31}$$

$$\frac{\partial \ln Z}{\partial \ln l_R} = \zeta(u) \tag{32}$$

where all derivatives have to be taken at fixed b, l and ϵ. Based on Padé–Borel summation of higher-order perturbation theory, a parametrization of the flow functions has been given in [24],

$$\zeta_n(u) = -u + \tfrac{5}{4}u^2 - a_1 u^3 + a_2 u^4 \tag{33}$$

$$\zeta(u) = -\tfrac{1}{4}u^2 + a_3 u^3 \tag{34}$$

$$\tilde{\beta}(u) = 4u^2 \frac{1 + a_4 u}{1 + a_5 u} \tag{35}$$

with the constants $a_1 = 3.6328$, $a_2 = 3.8953$, $a_3 = 0.043\,95$, $a_4 = 1.555$ and $a_5 = 3.5962$.

(Our notation differs somewhat from that of [24]: $u = 8u$, $\zeta_n = -\zeta_r$, $\zeta = \zeta_\phi$. We further note that recently some mistakes have been found [25] in the five-loop contributions to the renormalization factors. However, due to the remarkable stability of the Padé–Borel results this is not expected to yield serious changes in the parametrization of (33)–(35).)

Starting from arbitrary initial conditions set at $l_R = l$ we now integrate the flow equations to find functions $u(l_R)$ etc in analytic form. We then fix the final value of l_R by the condition

$$N_R = 1 \tag{36}$$

which implies that l_R is of order R_N. Resulting in the expressions

$$\alpha_N = l_0^2 \frac{e^{1.951u - 1.422u^2 + 0.734u^3}}{u^{1/4}(1 + 1.555u)^{1.369}} A_R(u, 1) \tag{37}$$

$$C_N/\mu^N = c_0 \frac{e^{2.101u - 1.434u^2 + 0.734u^3}}{u^{1/4}(1 + 1.555u)^{1.425}} A_C(u, 1)\,. \tag{38}$$

The renormalized coupling constant is implicitly determined by the equation

$$N = n_0 \frac{(1 + 1.555u)^{2.349}}{u^{0.730}} e^{1/2u - (1.951u - 1.422u^2 + 0.734u^3)}\,. \tag{39}$$

Here l_0, c_0, n_0 are non-universal fit parameters absorbing the initial conditions in the integration of the flow equations.

So far we have been concerned with the renormalization-group mapping. Calculation of the amplitudes is a straightforward exercise in renormalized perturbation theory. It yields

$$A_R(u, 1) = 1 - \tfrac{1}{2}u + O(u^2) \tag{40}$$

$$A_C(u, 1) = 1 + \tfrac{1}{2}u + O(u^2)\,. \tag{41}$$

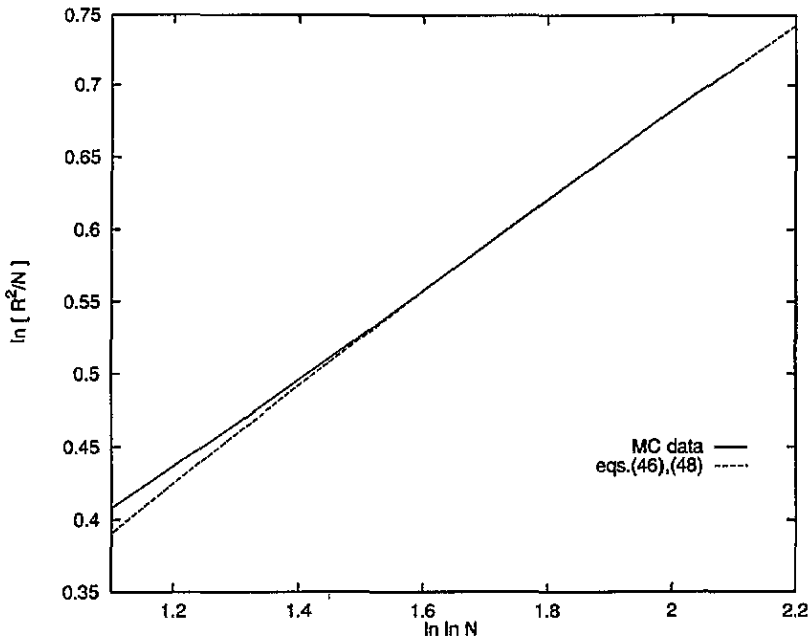

Figure 8. Fit to the swelling ratio α_N with $l_0 = 1.0436$ and $n_0 = 0.275$.

Equations (37)–(41) constitute our final result. From the derivation it should be clear that the calculation of the amplitudes is a problem well separated from the determination of the renormalization-group mapping. Indeed, within the minimal subtraction scheme it is the singular terms in expressions like (9) and (10) which determine the mapping, whereas the amplitudes result from regular terms.

We now compare to the Monte Carlo data. Fitting α_N in the range $300 \leqslant N \leqslant 4000$ we find $l_0 = 1.0436$ and $n_0 = 0.275$ (see figure 8). The same value for n_0 together with $c_0 = 0.864$ would also give an acceptable fit to C_N. But the best fit to the latter (see figure 9(*a*)) is obtained with $n_0 = 0.316$, $c_0 = 0.870$, and

$$p_c = 0.147\,622\,3 \pm 0.000\,000\,5\,. \tag{42}$$

The latter value for n_0 also gives an excellent fit to α_N, provided N is replaced by $N + n_1$ in the definition of α_N, with $n_1 = 0.56$ (see figure 9(*b*)). In the latter fit, $l_0 = 1.0466$. *A priori*, such a change would be well within the uncertainty intrinsic in the definition of N. But figure 7 and analogous plots of the dependence of u on l_R in the present scheme suggest that such a value of n_1 is somewhat large. We must note, however, that introducing n_1 we can account for $1/N$ corrections only in a very crude way [26]. We thus find agreement with the field-theoretic prediction, but there remains some room for further improvement in the region of short chains.

It is of some interest to note the range of the renormalized coupling resulting from our fit: $0.067 < u < 0.15$ for N in the range $4000 > N > 100$. Thus even for $N \approx 4000$ u is not particularly small. On the other hand, it is sufficiently small for the parametrizations of [24] to be justified.

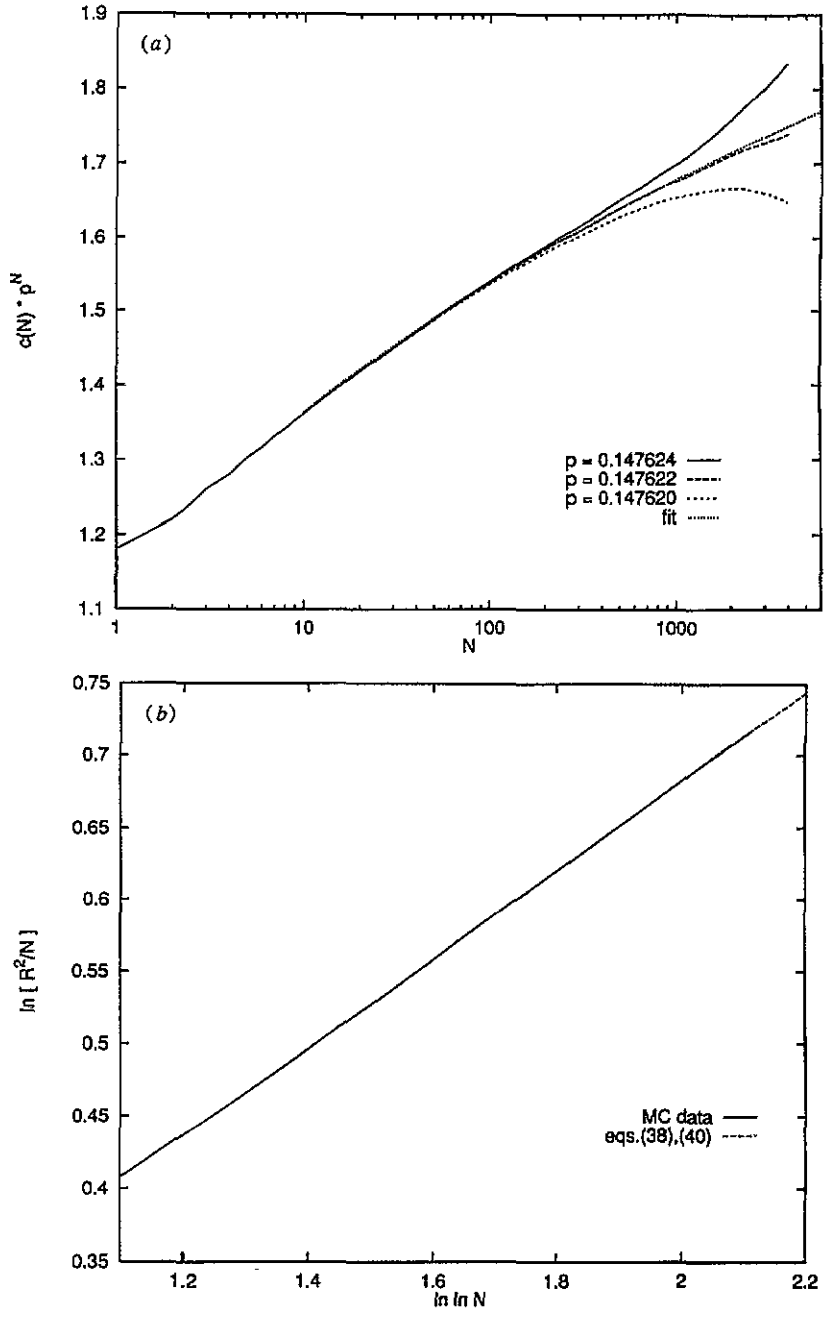

Figure 9. (*a*) Fit to C_N/μ^N with $c_0 = 0.870$ and $n_0 = 0.316$; (*b*) fit to α_N with the same $n_0 = 0.316$, with $l_0 = 1.0466$, and with $n_1 = 0.56$.

5. Discussion

We have seen that self-avoiding walks on the hypercubic lattice in four dimensions show clear logarithmic corrections. These corrections are in perfect agreement with the

predictions of the renormalization group, though they would be very poorly described by the asymptotically leading approximation. Thus claims [6–8] that these particular leading terms have been seen in simulations must be viewed with some reservation. On the other hand, our numerical results agree perfectly with simulations reported in [9], although the conclusion drawn in that paper seems to be wrong. Though our data are perfectly fitted by power laws in $\ln N$—in particular,

$$R_N^2/N \sim [\ln N]^{0.31} \tag{43}$$

these do not represent the asymptotic behaviour.

In order to understand the discrepancy with [7, 8], we have repeated their computation of $\langle N_R \rangle_p$ and their subsequent analysis, but with several modifications:

(i) using our algorithm, we calculated $\langle N_R \rangle_p$ not only for a single fixed value of R ($R = 7$ in [7, 8]), but for all $R < \sqrt{500}$;
(ii) due to the efficiency of our algorithm (and improved hardware) we have much higher statistics;
(iii) we use data much closer to the critical point: $p_c - p \geqslant 0.0012$ compared to $p_c - p \geqslant 0.018$; and
(iv) in the analysis we use our very accurate estimate for p_c.

Assuming that the decay of the two-point function is dominated by the smallest mass m in the model (the inverse correlation length ξ), the authors of [7, 8] obtain

$$\langle N_R \rangle_p \sim R \frac{dm}{dp} \tag{44}$$

with

$$m \equiv 1/\xi \sim \sqrt{p_c - p}\,[\ln(p_c - p)]^{-\mathcal{N}} \qquad \mathcal{N} = \tfrac{1}{8}. \tag{45}$$

Thus, $\langle N_R \rangle_p / R$ should be a function of p alone, independent of R. Our data shown in figure 10 clearly demonstrate that this is only true for $R \gg \xi$, while

$$\langle N_R \rangle_p \sim R \ln R \tag{46}$$

for $R < \xi$. This is not surprising: the decay of the correlation function should be dominated by the smallest mass only for $R \gg \xi$, while effects of the effective coupling should be visible at shorter-distances. Indeed, keeping R fixed while $p \to p_c$ we encounter the region where the data should be analysed via a short-distance expansion, and (44) is no longer justified. According to figure 10, $R = 7$ is not yet in the regime where (44) holds for the range of p considered in [7]. This already gives a first indication that this coupling is larger than anticipated in [7] (we might add that the fluctuations seen in figure 10 are not statistical, but are lattice effects).

In figure 11 we show our data for $R = 7, \sqrt{150}$ and $\sqrt{500}$ together with those of [7], and with the mean-field prediction

$$\frac{\langle N_R \rangle_p}{R} \propto \frac{1}{\sqrt{p_c - p}}. \tag{47}$$

On the one hand we see that the slopes deviate strongly from the mean-field prediction, much more than they differ between different values of R. On the other hand, we see the dramatic effect of a wrong choice of p_c. Indeed, while we use our value of p_c when plotting our own data, we show the data of [7] twice: once plotted using our p_c, and once using their own estimate of p_c. We see that the latter reduces the deviation from the mean-field considerably. Thus we see that the logarithmic corrections are indeed larger than estimated

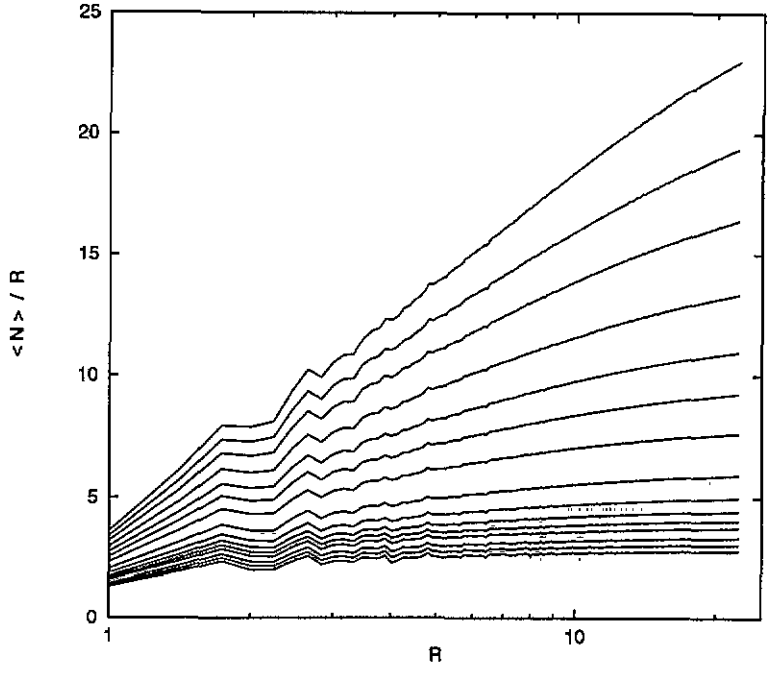

Figure 10. Average chain lengths at fixed p against their end-to-end distance R. Actually, the ratio $\langle N_R \rangle_p / R$ is plotted. The values of $\ln(1/p)$ (from top to bottom) are: 1.9143, 1.915, 1.916, 1.918, 1.921, 1.925, 1.932, 1.948, 1.966, 1.984, 2.002, 2.021, 2.066, 2.100 and 2.150.

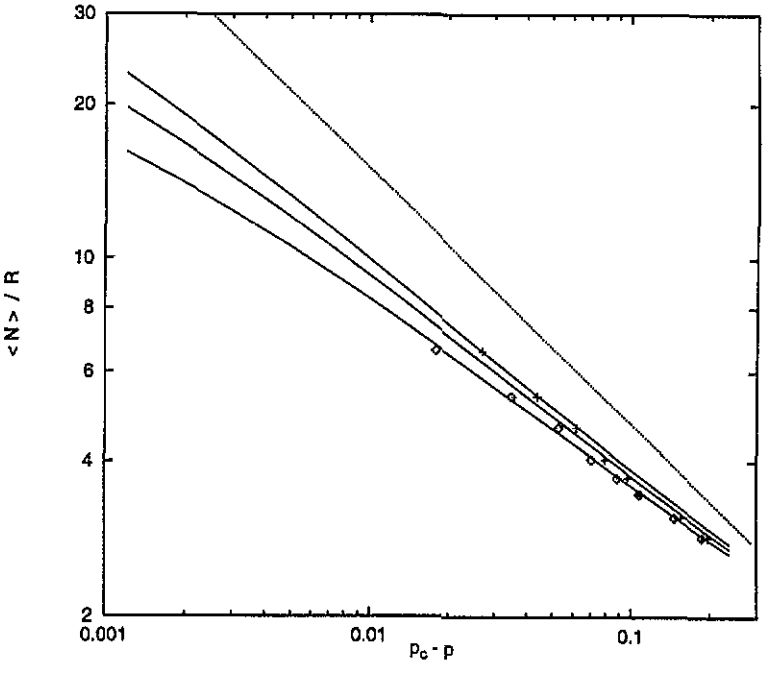

Figure 11. Full curves: $\langle N_R \rangle_p / R$ against $p_c - p$ for $R = 7$, 12.25 and 22.36 (from bottom to top); dotted curve: slope $\langle N_R \rangle_p \propto (p_c - p)^{-1/2}$ predicted by mean-field theory; ($\Diamond$) data of [7] (for $R = 7$), using our value of p_c; (+) data of [7], using their value of p_c.

in [7] (in spite of the fact that alone the too small value of R would have led to their *over*estimation!), but the systematic uncertainties and the lack of higher-order predictions from field theory prevent a more detailed analysis. The same comments should hold for the data of [8], as this author used the same values of R and of p as [7], and his estimated p_c was even further from our estimate.

To what chain lengths would we have to go in order to see the asymptotic behaviour R_N^2/N, $C_N/\mu^N \sim [\ln N]^{1/4}$? Our renormalization-group calculation can easily be extended to larger N and show that (43) would no longer give a good fit above $N = 10^4$, but even at $N = 10^7$ the effective exponent is ≈ 0.285 instead of $\frac{1}{4}$.

The analysis in the field-theoretic framework stresses the importance of a good quantitative form of the renormalization-group mapping. For the amplitudes then a low-order approximation seems sufficient. This supports previous findings, both in polymer physics [13] and in the physics of liquid helium [14]. If a good form of the mapping were missing, this would justify the often expressed pessimism about the possibility of seeing, for example, logarithmic corrections. Such a situation prevails for θ-polymers in three dimensions. There only leading terms in the sense of (5) and (6) have been computed [27], and they disagree badly with simulations [11]. Although the disagreement is even worse than with the leading terms in the present case, one might suspect that also the poor representation of the renormalization group mapping employed is at the root of the problem.

The present analysis showed large subleading corrections because of the rather large value of the renormalized coupling constant, even for our longest chains. This raises the question of whether the asymptotic behaviour could be seen for much shorter chains in models with weaker repulsion between chains. Two such models come immediately to mind: chains with attraction between neighbouring sites (θ polymers above T_θ), and the Domb–Joyce model [28]. In the latter, $n > 1$ monomers can occupy the same site, but the contribution to the partition function gets a weight $(1 - w)^{n-1}$ for each multiple occupancy. For sufficiently small w one is arbitrarily close to the free case, and also the renormalized coupling constant should be small.

Acknowledgments

This work was supported by DFG, SFB 237, and by the Graduiertenkolleg 'Feldtheoretische un numerische Methoden in der Elementarteilchen- und Statistischen Physik'.

References

[1] de Gennes P G 1979 *Scaling Concepts in Polymer Physics* (Ithaca, NY: Cornell University Press)
[2] McKenzie S 1979 *J. Phys. A: Math. Gen.* **12** L267
[3] Guttmann A J 1978 *J. Phys. A: Math. Gen.* **11** L103; 1981 *J. Phys. A: Math. Gen.* **14** 233
[4] MacDonald D, Hunter D L, Kelly K and Jan N 1992 *J. Phys. A: Math. Gen.* **25** 1429
[5] MacDonald D, Hunter D L, Kelly K and Jan N 1993 Private communication
[6] Havlin S and Ben-Avraham D 1982 *J. Phys. A: Math. Gen.* **15** L317
[7] de Carvalho C A, Caracciolo S and Fröhlich J 1983 *Nucl. Phys.* B **215** 209
[8] van Rensburg E J J 1988 *J. Phys. G: Nucl. Phys.* **14** 397
[9] Rapaport D C 1984 *Phys. Rev.* B **30** 2906
[10] Hegger R *PhD thesis* (to be published)
[11] Grassberger P and Hegger R 1994 *J. Chem. Phys.* submitted
[12] Duplantier B 1986 *Nucl. Phys.* B **275** 319
[13] Schäfer L 1984 *Macromolecules* **17** 1353; 1990 *Coll. Poly. Sci.* **268** 995
[14] Krause H J, Schloms R and Dohm V 1990 *Z. Phys.* B **79** 287; **80** 313
[15] des Cloizeaux J 1981 *J. Physique* **42** 635

[16] Madras N and Sokal A D 1988 *J. Stat. Phys.* **50** 109
[17] Wall F T and Erpenbeck J J 1959 *J. Chem. Phys.* **30** 634, 637
[18] Redner S and Reynolds P J 1981 *J. Phys. A: Math. Gen.* **14** 2679
[19] Grassberger P 1993 *J. Phys. A: Math. Gen.* **26** 1023, 2769
[20] Grassberger P and Hegger R 1994 *Preprint*
[21] Beretti A and Sokal A D 1985 *J. Stat. Phys.* **40** 483
[22] Duplantier B 1986 *J. Physique* **47** 569
[23] des Cloizeaux J and Jannink G 1990 *Polymers in Solution: Their Modelling and Structure* (Oxford: Clarendon)
[24] Schloms R and Dohm V 1989 *Nucl. Phys.* B **328** 639
[25] Kleinert H, Neu J, Schulte-Frohlinde V, Chetyrkin K G and Larin S A 1991 *Phys. Lett.* **272B** 39
[26] Krüger B and Schäfer L 1994 *J. Physique. I* **4** 757
[27] Duplantier B 1987 *J. Chem. Phys.* **86** 4233
[28] Domb C and Joyce G S 1972 *J. Phys. C: Solid State Phys.* **5** 956